Available online at www.sciencedirect.com
SCIENCE DIRECT®
PERGAMON
International Journal of Heat and Mass Transfer 46 (2003) 4935–4948
International Journal of HEAT and MASS TRANSFER
www.elsevier.com/locate/ijhmt

One-dimensional drift-flux model and constitutive equations for relative motion between phases in various two-phase flow regimes

Takashi Hibiki [a,1], Mamoru Ishii [b,*]

[a] Research Reactor Institute, Kyoto University, Kumatori, Sennan, Osaka 590-0494, Japan
[b] School of Nuclear Engineering, Purdue University, 400 Central Drive, West Lafayette, IN 47907-2017, USA

Received 30 January 2003

Abstract

In view of the practical importance of the drift-flux model for two-phase flow analysis in general and in the analysis of nuclear-reactor transients and accidents in particular, the kinematic constitutive equation for the drift velocity has been studied for various two-phase flow regimes. The constitutive equations that specify the relative motion between phases in the drift-flux model has been derived by taking into account the interfacial geometry, the body-force field, the shear stresses, the interfacial momentum transfer and the wall friction, since these macroscopic effects govern the relative velocity between phases. A comparison of the models with existing experimental data shows a satisfactory agreement.

Keywords: Drift flux model; Distribution parameter; Drift velocity; Gas–liquid flow; Multiphase flow; Void fraction

1. Introduction

Two-phase flows always involve some relative motion of one phase with respect to the other; therefore, a two-phase-flow problem should be formulated in terms of two velocity fields. A general transient two-phase-flow problem can be formulated by using a two-fluid model [1,2] or a drift-flux model [3,4], depending on the degree of the dynamic coupling between the phases. In the two-fluid model, each phase is considered separately; hence the model is formulated in terms of two sets of conservation equations governing the balance of mass, momentum, and energy of each phase. However, an introduction of two momentum equations in a formulation, as in the case of the two-fluid model, presents considerable difficulties because of mathematical complications and of uncertainties in specifying interfacial interaction terms between two phases [1,2]. Numerical instabilities caused by improper choice of interfacial-interaction terms in the phase-momentum equations are common; therefore careful studies on the interfacial constitutive equations are required in the formulation of the two-fluid model.

These difficulties associated with a two-fluid model can be significantly reduced by formulating two-phase problems in terms of the drift-flux model, in which the motion of the whole mixture is expressed by the mixture momentum equation and the relative motion between phases is taken into account by a kinematic constitutive equation. Therefore, the basic concept of the drift-flux model is to consider the mixture as a whole, rather than as two separated phases. The formulation of the drift-flux model based on the mixture balance equations is simpler than the two-fluid model based on the separate balance equations for each phase. The most important assumption associated with the drift-flux model is that the dynamics of two phases can be expressed by the

* Corresponding author. Tel.: +1-765-494-4587; fax: +1-765-494-9570.
E-mail addresses: hibiki@rri.kyoto-u.ac.jp (T. Hibiki), ishii@ecn.purdue.edu (M. Ishii).
[1] Tel.: +81-724-51-2373; fax: +81-724-51-2461.

0017-9310/$ - see front matter
doi:10.1016/S0017-9310(03)00322-3

Nomenclature

A	cross-sectional area
c	coefficient
C_0	distribution parameter
C_∞	asymptotic value of C_0
C_D	drag coefficient in multi-bubble system
C'_D	drag coefficient in multi-bubble system
$C_{D\infty}$	drag coefficient in single-bubble system
C_v	distribution parameter for momentum
D	diameter of a pipe
D_H	hydraulic equivalent diameter of flow channel
D_{Sm}	Sauter mean diameter
$\widetilde{D}_{Sm}$	non-dimensional Sauter mean diameter
E_V	prediction error
E_M	prediction error
F	quantity
f	friction factor
$f(\langle\alpha_g\rangle)$	function
F_D	drag force
g	gravitational acceleration
h	enthalpy
$\bar{h}$	mean enthalpy
j	superficial velocity
Lo	Laplace length
$\widetilde{Lo}$	non-dimensional Laplace length
M^d	interfacial shear force
M_F	frictional pressure gradient in multi-bubble system
$M_{F\infty}$	frictional pressure gradient in single-bubble system
M_i	interfacial drag
M_τ	gradient of normal components of stress tensor in axial direction
p	pressure
Q	volume flow rate
q	conduction heat flux
q^T	turbulent heat flux
q''_W	wall heat flux
R	pipe radius
r_b	bubble radius
Re	Reynolds number
$\widetilde{Re}$	bubble Reynolds number
Re^*	Reynolds number in multi-bubble system
Re^*_∞	Reynolds number in single-bubble system
t	time
v	velocity
$\bar{v}$	mean velocity
V_{gj}	drift velocity of gas phase
$\overline{V_{gj}}$	mean drift velocity of gas phase
v_r	relative velocity between phases in multi-bubble system
$v_{r\infty}$	relative velocity between phases in single-bubble system
z	axial distance

Greek symbols

α	phase fraction or void fraction
Γ	mass source
Δh_{gf}	enthalpy difference
$\Delta\rho$	density difference between phases
ε	energy dissipation rate per unit mass
μ	viscosity
ν	kinematic viscosity
ξ_h	heated perimeter
ρ	density
σ	surface tension
$\bar{\bar{\tau}}$	viscous stress
$\bar{\bar{\tau}}^T$	turbulent diffusion flux of momentum
τ_i	interfacial shear stress
τ_{zz}	normal viscous stress
τ^T_{zz}	normal turbulent stress
Φ^μ	energy dissipation
ψ	property

Subscripts

f	liquid phase
g	gas phase
i	value at interface
k	k phase
l	laminar flow
m	weighted mean mixture property
t	turbulent flow
w	value at wall
z	z-component

Mathematical symbols

$\langle\ \rangle$	area averaged value
$\langle\langle\ \rangle\rangle$	weighted mean value
COV	covariance

mixture-momentum equation with the kinematic constitutive equation specifying the relative motion between phases. The use of the drift-flux model is appropriate when the motions of two phases are strongly coupled.

In the drift-flux model, the velocity fields are expressed in terms of the mixture center-of-mass velocity and the drift velocity of the vapor phase, which is the vapor velocity with respect to the volume center of the mixture. The effects of thermal non-equilibrium are accommodated in the drift-flux model by a constitutive equation for phase change that specifies the rate of mass transfer per unit volume. Since the rates of mass and momentum transfer at the interfaces depend on the structure of two-phase flows, these constitutive equa-

tions for the drift velocity and the vapor generation are functions of flow regimes.

The drift-flux model is an approximate formulation in comparison with the more rigorous two-fluid formulation. However, because of its simplicity and applicability to a wide range of two-phase-flow problems of practical interest, the drift-flux model is of considerable importance. In particular, the model is useful for transient thermohydraulic and accident analyses of both LWR's and LMFBR's [4]. In view of the practical importance of the drift-flux model for two-phase-flow analyses, the constitutive equations that specify the relative motion between phases in the drift-flux model have been derived by Ishii [4] by taking into account the interfacial geometry, the body-force field, shear stresses, and the interfacial momentum transfer, since these macroscopic effects govern the relative velocity between phases. To derive the simplified one-dimensional constitutive equations specifying the one-dimensional drift velocity, Ishii [4] assumed that the average drift velocity due to the local slip can be predicted by the same expression as the local constitutive relations, provided the local void fraction and the difference of the stress gradient are replaced by average values. The validity of the constitutive equations developed by Ishii [4] has been supported by various experimental data over various flow regimes and a wide range of flow parameters. However, it is anticipated that such simplified one-dimensional constitutive equations may not give a good prediction in some extreme flow conditions such as very high liquid flow and microgravity conditions where the effect of the wall shear stress on the relative velocity between phases may become significant. From this point of view, the purpose of the present study is to derive more rigorous constitutive equations specifying the one-dimensional drift velocity by taking into account the wall shear stress. The derived constitutive equations are validated by existing experimental data.

2. One-dimensional drift-flux model

Averaging over the cross-sectional area is useful for complicated engineering problems involving fluid flow and heat transfer, since field equations can be reduced to quasi-one-dimensional forms. By area averaging, the information on changes of variables in the direction normal to the mean flow within a channel is basically lost; therefore, the transfer of momentum and energy between the wall and the fluid should be expressed by empirical correlations or by simplified models. The rational approach to obtain a one-dimensional model is to integrate the three-dimensional model over a cross-sectional area and then to introduce proper mean values.

A simple area average over the cross-sectional area, A, is defined by

$$\langle F\rangle = \frac{1}{A}\int_A F\,\mathrm{d}A, \tag{1}$$

and the void-fraction-weighted mean value is given by

$$\langle\langle F_k\rangle\rangle = \langle\alpha_k F_k\rangle/\langle\alpha_k\rangle. \tag{2}$$

Here, $\langle F\rangle$ and α_k are a simple area average of a quantity and the conventional time- (or ensemble)-averaged local void fraction, respectively. The component k denotes either the liquid (k = f) or the gas phase (k = g).

In the present analysis, the density of each phase, ρ_g and ρ_f within any cross-sectional area is considered to be uniform, so that $\rho_k = \langle\langle\rho_k\rangle\rangle$. For most practical two-phase flow problems, this assumption is valid since the transverse pressure gradient within a channel is relatively small. The detailed analysis without this approximation appears in Ref. [5]. Under the above simplifying assumption, the average mixture density is given by

$$\langle\rho_m\rangle \equiv \langle\alpha_g\rangle\rho_g + (1-\langle\alpha_g\rangle)\rho_f. \tag{3}$$

The axial component of the weighted mean velocity of phase k is

$$\langle\langle v_k\rangle\rangle = \frac{\langle\alpha_k v_k\rangle}{\langle\alpha_k\rangle} = \frac{\langle j_k\rangle}{\langle\alpha_k\rangle}. \tag{4}$$

Then, the mixture velocity is defined by

$$\overline{v_m} \equiv \frac{\langle\rho_m v_m\rangle}{\langle\rho_m\rangle} = \frac{\langle\alpha_g\rangle\rho_g\langle\langle v_g\rangle\rangle + (1-\langle\alpha_g\rangle)\rho_f\langle\langle v_f\rangle\rangle}{\langle\rho_m\rangle}, \tag{5}$$

and the volumetric flux is given by

$$\langle j\rangle \equiv \langle j_g\rangle + \langle j_f\rangle = \langle\alpha_g\rangle\langle\langle v_g\rangle\rangle + (1-\langle\alpha_g\rangle)\langle\langle v_f\rangle\rangle. \tag{6}$$

The mean mixture enthalpy should also be weighted by the density; thus,

$$\overline{h_m} \equiv \frac{\langle\rho_m h_m\rangle}{\langle\rho_m\rangle} = \frac{\langle\alpha_g\rangle\rho_g\langle\langle h_g\rangle\rangle + (1-\langle\alpha_g\rangle)\rho_f\langle\langle h_f\rangle\rangle}{\langle\rho_m\rangle}. \tag{7}$$

The vapor drift velocity of a gas phase is defined as the velocity of the dispersed phase with respect to the volume center of the mixture:

$$V_{gj} \equiv v_g - j. \tag{8}$$

The appropriate mean drift velocity is defined by

$$\begin{aligned}\overline{V_{gj}} &\equiv \langle\langle v_g\rangle\rangle - \langle j\rangle = (1-\langle\alpha_g\rangle)(\langle\langle v_g\rangle\rangle - \langle\langle v_f\rangle\rangle)\\ &= \langle\langle V_{gj}\rangle\rangle + (C_0-1)\langle j\rangle,\end{aligned} \tag{9}$$

where

$$\langle\langle V_{gj}\rangle\rangle \equiv \frac{\langle\alpha_g V_{gj}\rangle}{\langle\alpha_g\rangle}, \tag{10}$$

and

$$C_0 \equiv \frac{\langle\alpha_g j\rangle}{\langle\alpha_g\rangle\langle j\rangle}. \tag{11}$$

The experimental determination of the above-defined drift velocity is possible if the volume flow rate of each

phase, Q_k and the mean void fraction $\langle \alpha_g \rangle$ are measured. This is because Eq. (9) can be transformed into

$$\overline{V_{gj}} = \frac{\langle j_g \rangle}{\langle \alpha_g \rangle} - (\langle j_g \rangle + \langle j_f \rangle), \tag{12}$$

where $\langle j_k \rangle$ is given by $\langle j_k \rangle = Q_k/A$. Furthermore, the present definition of the drift velocity can also be used for annular two-phase flows. Under the definitions of various velocity fields, we obtain several important relations, such as

$$\langle\langle v_g \rangle\rangle = \overline{v_m} + \frac{\rho_f}{\langle \rho_m \rangle} \overline{V_{gj}}, \tag{13}$$

$$\langle\langle v_f \rangle\rangle = \overline{v_m} - \frac{\langle \alpha_g \rangle}{1 - \langle \alpha_g \rangle} \frac{\rho_g}{\langle \rho_m \rangle} \overline{V_{gj}}, \tag{14}$$

and

$$\langle j \rangle = \overline{v_m} + \frac{\langle \alpha_g \rangle (\rho_f - \rho_g)}{\langle \rho_m \rangle} \overline{V_{gj}}. \tag{15}$$

In the drift-flux formulation, a problem is solved for $\langle \alpha_g \rangle$ and $\overline{v_m}$ with a given constitutive relation for $\overline{V_{gj}}$. Thus, Eqs. (13) and (14) can be used to recover a solution for the velocity of each phase after a problem is solved.

By area-averaging three-dimensional form of the drift-flux model [2] and using the various mean values, we obtain:

Mixture continuity equation:

$$\frac{\partial \langle \rho_m \rangle}{\partial t} + \frac{\partial}{\partial z}(\langle \rho_m \rangle \overline{v_m}) = 0. \tag{16}$$

Continuity equation for dispersed phase:

$$\frac{\partial \langle \alpha_g \rangle \rho_g}{\partial t} + \frac{\partial}{\partial z}(\langle \alpha_g \rangle \rho_g \overline{v_m}) = \langle \Gamma_g \rangle - \frac{\partial}{\partial z}\left(\frac{\langle \alpha_g \rangle \rho_g \rho_f}{\langle \rho_m \rangle} \overline{V_{gj}} \right). \tag{17}$$

Mixture momentum equation:

$$\begin{aligned} &\frac{\partial \langle \rho_m \rangle \overline{v_m}}{\partial t} + \frac{\partial}{\partial z}(\langle \rho_m \rangle \overline{v_m}^2) \\ &= -\frac{\partial}{\partial z}\langle p_m \rangle + \frac{\partial}{\partial z}\langle \tau_{zz} + \tau_{zz}^T \rangle - \langle \rho_m \rangle g_z - \frac{f_m}{2D}\langle \rho_m \rangle \overline{v_m}|\overline{v_m}| \\ &\quad - \frac{\partial}{\partial z}\left[\frac{\langle \alpha_g \rangle \rho_g \rho_f}{(1 - \langle \alpha_g \rangle)\langle \rho_m \rangle} \overline{V_{gj}}^2 \right] - \frac{\partial}{\partial z} \sum_k \mathrm{COV}(\alpha_k \rho_k v_k v_k). \end{aligned} \tag{18}$$

Mixture enthalpy-energy equation:

$$\begin{aligned} &\frac{\partial \langle \rho_m \rangle \overline{h_m}}{\partial t} + \frac{\partial}{\partial z}(\langle \rho_m \rangle \overline{h_m v_m}) \\ &= -\frac{\partial}{\partial z}\langle q + q^T \rangle + \frac{q''_W \xi_h}{A} - \frac{\partial}{\partial z}\frac{\langle \alpha_g \rangle \rho_g \rho_f}{\langle \rho_m \rangle} \Delta h_{gf} \overline{V_{gj}} \\ &\quad - \frac{\partial}{\partial z}\left[\frac{\langle \alpha_g \rangle \rho_g \rho_f}{\langle \rho_m \rangle} \Delta h_{gf} \overline{V_{gj}} \right] - \frac{\partial}{\partial z} \sum_k \mathrm{COV}(\alpha_k \rho_k h_k v_k) \\ &\quad + \frac{\partial \langle \rho_m \rangle}{\partial t} + \left[\overline{v_m} + \frac{\langle \alpha_g \rangle (\rho_f - \rho_g)}{\langle \rho_m \rangle} \overline{V_{gj}} \right] \frac{\partial \langle \rho_m \rangle}{\partial z} + \langle \Phi_m^\mu \rangle. \end{aligned} \tag{19}$$

Here, $\tau_{zz} + \tau_{zz}^T$ denotes the normal components of the stress tensor in the axial direction and Δh_{gf} is the enthalpy difference between phases; thus, $\Delta h_{gf} = \langle\langle h_g \rangle\rangle - \langle\langle h_f \rangle\rangle$. g_z, ξ_h and Φ_m^μ are the z-component of the gravitational acceleration, the heated perimeter and the mixture-energy dissipation, respectively. The covariance terms represent the difference between the average of a product and the product of the average of two variables such that $\mathrm{COV}(\alpha_k \rho_k \psi_k v_k) \equiv \langle \alpha_k \rho_k \psi_k (v_k - \langle\langle v_k \rangle\rangle) \rangle$ where ψ_k represents the property of k phase. If the profile of either ψ_k or v_k is flat, then the covariance term reduces to zero. The term represented by $f_m \langle \rho_m \rangle \overline{v_m}|v_m|/(2D)$ in Eq. (18) is the two-phase frictional pressure drop. We note here that the effects of the mass, momentum, and energy diffusion associated with the relative motion between phases appear explicitly in the field equations are expressed in terms of the mixture velocity. These effects of diffusions in the present formulation are expressed in terms of the drift velocity of the dispersed phase, $\overline{V_{gj}}$. This may be formulated in a functional form as

$$\overline{V_{gj}} = \overline{V_{gj}}(\langle \alpha_g \rangle, \langle p_m \rangle, g_z, \overline{v_m}, \text{etc.}). \tag{20}$$

To take into account the mass transfer across the interfaces, a constitutive equation for mass source for gas phase, $\langle \Gamma_g \rangle$, should also be given. In a functional form, this phase-change constitutive equation may be written as

$$\langle \Gamma_g \rangle = \langle \Gamma_g \rangle \left(\langle \alpha_g \rangle, \langle p_m \rangle, \overline{v_m}, \frac{\partial \langle p_m \rangle}{\partial t}, \text{etc.} \right). \tag{21}$$

The above formulation can be extended to non-dispersed two-phase flows, such as an annular flow, provided a proper constitutive relation for a drift velocity of one of the phases is given. In what follows, the constitutive equations specifying the one-dimensional drift velocity will be derived by taking into account the wall shear stress.

3. One-dimensional drift velocity

3.1. Dispersed two-phase flow

3.1.1. Relative motion in single-bubble system in confined channel

Recently, Tomiyama et al. [6] derived the relative velocity in a confined channel by taking into account the effect of a frictional pressure gradient due to a liquid flow. In what follows, we shall summarize the result in a simple form useful for the development of the drift constitutive equation in multi-bubble systems.

By denoting the relative velocity of a single bubble in an infinite medium by $v_{r\infty} = v_g - v_{f\infty}$, we define the drag coefficient by

$$C_{D\infty} \equiv -\frac{2F_D}{\rho_f v_{r\infty}|v_{r\infty}|\pi r_b^2}, \tag{22}$$

where F_D and r_b are the drag force and the radius of a bubble, respectively. Clift et al. [7] indicated that the effect of the pipe wall on $C_{D\infty}$ is negligible if the ratio of the bubble diameter, r_d to the pipe radius, R, is less than 0.125. Hence, assuming the negligible effect of the pipe wall on $C_{D\infty}$, the momentum equation for the fully-developed liquid flow can be written as

$$0 = -\frac{dp}{dz} - M_{F\infty} - \rho_f g_z, \tag{23}$$

where $M_{F\infty}$ is the frictional pressure gradient given by

$$M_{F\infty} = \frac{f}{2D}\rho_f \langle v_f \rangle^2, \tag{24}$$

where f and D are the wall friction factor and the pipe diameter, respectively. The momentum equation for the bubble can be written as

$$0 = -\frac{dp}{dz} - \frac{3}{8}\frac{C_{D\infty}\rho_f v_{r\infty}|v_{r\infty}|}{r_b} - \rho_g g_z. \tag{25}$$

Then from Eqs. (23) and (25), we obtain

$$v_{r\infty}|v_{r\infty}| = \frac{8}{3}\frac{r_b}{C_{D\infty}\rho_f}(\Delta\rho g_z + M_{F\infty}). \tag{26}$$

3.1.2. One-dimensional relative velocity of dispersed flow in confined channel

For a dispersed two-phase flow, the averaged interfacial drag term could be given approximately by [8]

$$\langle M_{ig} \rangle = -\frac{3}{8}\frac{C_D}{\langle r_b \rangle}\langle \alpha_g \rangle \rho_f \langle v_r \rangle |\langle v_r \rangle|. \tag{27}$$

The above approximate form is obtained based on the experimental observation that the local relative velocity, v_r is comparatively uniform across a flow channel [9].

The one-dimensional interfacial drag force of the gas phase, $\langle M_{ig} \rangle$, can be derived from the one-dimensional momentum equation by integrating the three-dimensional momentum equation over the flow channel. Under the assumption that the averaged pressure in the bulk fluid and at the interface is approximately the same, we obtain the three-dimensional momentum equation as

$$\begin{aligned}&\frac{\partial \alpha_k \rho_k \overrightarrow{v_k}}{\partial t} + \nabla\cdot(\alpha_k\rho_k\overrightarrow{v_k}\overrightarrow{v_k}) \\ &\quad = -\alpha_k\nabla p_k + \nabla\cdot\left\{\alpha_k\left(\overline{\overline{\tau_k}} + \overline{\overline{\tau_k}}^T\right)\right\} + \alpha_k\rho_k\vec{g} \\ &\qquad + \overrightarrow{v_{ki}}\Gamma_k + \overrightarrow{M_{ik}} - \nabla\alpha_k\cdot\tau_i,\end{aligned} \tag{28}$$

where $\overline{\overline{\tau}}$, $\overline{\overline{\tau}}^T$ and τ_i are the viscous stresses, the turbulent diffusion flux of momentum and the interfacial shear stress, respectively. The subscript of ki denotes the value at the interface for phase k.

By area-averaging Eq. (28), and making some simplifications, which are applicable to most practical problems, the following one-dimensional momentum equation can be obtained [8]:

$$\begin{aligned}&\frac{\partial}{\partial t}\langle\alpha_k\rangle\rho_k\langle\langle v_k\rangle\rangle + \frac{\partial}{\partial z}C_{vk}\langle\alpha_k\rangle\rho_k\langle\langle v_k\rangle\rangle^2 \\ &\quad = -\langle\alpha_k\rangle\frac{\partial}{\partial z}\langle\langle p_k\rangle\rangle + \frac{\partial}{\partial z}\langle\alpha_k\rangle\langle\langle\tau_{kzz} + \tau^T_{kzz}\rangle\rangle \\ &\qquad - \frac{4\alpha_{kw}\tau_{kw}}{D} - \langle\alpha_k\rangle\rho_k g_z + \langle\Gamma_k\rangle\langle\langle v_{ki}\rangle\rangle + \langle M^d_k\rangle,\end{aligned} \tag{29}$$

where α_{kw} and τ_{kw} are the mean void fraction at the wall and the wall shear stress, respectively. $\langle M^d_k \rangle$ is the total interfacial shear force given by

$$\langle M^d_k \rangle = \langle M_{ik} - \nabla\alpha_k\cdot\tau_i \rangle. \tag{30}$$

In the convective term, the distribution parameter for the k-phase momentum, C_{vk}, appears due to the difference between the average of a product of variables and the product of averaged variables.

Under the steady-state condition without phase change ($\langle\Gamma_k\rangle = 0$) and with negligible transverse pressure gradient, i.e., $\langle\langle p_f\rangle\rangle = \langle\langle p_g\rangle\rangle = \langle\langle p_m(z)\rangle\rangle$, and the assumption that the averaged pressure and stress in the bulk fluid and at the interface are approximately the same, the one-dimensional momentum equation for phase k can be reduced from Eq. (29) to

$$\begin{aligned}0 = &-\langle\alpha_k\rangle\frac{\partial}{\partial z}\langle\langle p_m\rangle\rangle - \langle\alpha_k\rangle\langle M_{\tau k}\rangle - \frac{4\alpha_{kw}\tau_{kw}}{D} \\ &- \langle\alpha_k\rangle\rho_k g_z + \langle M_{ik}\rangle,\end{aligned} \tag{31}$$

where

$$\langle M_{\tau k}\rangle \equiv \frac{\partial}{\partial z}\langle\langle\tau_{kzz} + \tau^T_{kzz}\rangle\rangle. \tag{32}$$

Consequently, we obtain

$$\begin{aligned}0 = &-\langle\alpha_g\rangle\frac{\partial}{\partial z}\langle\langle p_m\rangle\rangle - \langle\alpha_g\rangle\langle M_{\tau g}\rangle - \frac{4\alpha_{gw}\tau_{gw}}{D} \\ &- \langle\alpha_g\rangle\rho_g g_z + \langle M_{ig}\rangle,\end{aligned} \tag{33}$$

and

$$\begin{aligned}0 = &-\langle\alpha_f\rangle\frac{\partial}{\partial z}\langle\langle p_m\rangle\rangle - \langle\alpha_f\rangle\langle M_{\tau f}\rangle - \frac{4\alpha_{fw}\tau_{fw}}{D} \\ &- \langle\alpha_f\rangle\rho_f g_z + \langle M_{if}\rangle.\end{aligned} \tag{34}$$

However, from the macroscopic jump condition at the interface, we have

$$\langle M_{ig}\rangle + \langle M_{if}\rangle = 0. \tag{35}$$

Thus, by eliminating the interfacial forces from the above two equations, we get

$$\frac{\partial}{\partial z}\langle\langle p_m\rangle\rangle = -\rho_m g_z - \langle M_{\tau m}\rangle - \frac{4\alpha_{gw}\tau_{gw}}{D} - \frac{4\alpha_{fw}\tau_{fw}}{D}, \tag{36}$$

where

$$\langle M_{\tau m}\rangle = \langle\alpha_g\rangle\langle M_{\tau g}\rangle + \langle\alpha_f\rangle\langle M_{\tau f}\rangle. \tag{37}$$

From Eqs. (33) and (36), we obtain

$$\langle M_{ig}\rangle = -\langle\alpha_g\rangle\left[\Delta\rho g_z(1-\langle\alpha_g\rangle) + (\langle M_{\tau m}\rangle - \langle M_{\tau g}\rangle) + \frac{4\alpha_{fw}\tau_{fw}}{D} - \frac{1-\langle\alpha_g\rangle}{\langle\alpha_g\rangle}\frac{4\alpha_{gw}\tau_{gw}}{D}\right]. \quad (38)$$

Without phase change, $\alpha_{gw} \cong 0$ and $\alpha_{fw} \cong 1$. Thus, Eq. (38) can be simplified to

$$\langle M_{ig}\rangle = -\langle\alpha_g\rangle\left[\Delta\rho g_z(1-\langle\alpha_g\rangle) + (1-\langle\alpha_g\rangle)(\langle M_{\tau f}\rangle - \langle M_{\tau g}\rangle) + \frac{4\tau_{fw}}{D}\right]. \quad (39)$$

For a fully developed vertical flow, the stress distribution in the fluid and in the dispersed phase should be similar and the values of $\langle M_{\tau g}\rangle$ and $\langle M_{\tau f}\rangle$ are generally small [4]; thus the effect of the shear gradient on the mean local drift velocity can be neglected.

$$\langle M_{ig}\rangle \approx -\langle\alpha_g\rangle\left[\Delta\rho g_z(1-\langle\alpha_g\rangle) + \frac{4\tau_{fw}}{D}\right] = -\langle\alpha_g\rangle[\Delta\rho g_z(1-\langle\alpha_g\rangle) + M_F], \quad (40)$$

where

$$M_F \equiv \frac{4\tau_{fw}}{D} = \left(-\frac{dp}{dz}\right)_F. \quad (41)$$

Substituting Eq. (41) into Eq. (27) yields

$$\langle v_r\rangle|\langle v_r\rangle| = \frac{8}{3}\frac{\langle r_b\rangle}{C_D\rho_f}\{\Delta\rho g_z(1-\langle\alpha_g\rangle) + M_F\}. \quad (42)$$

From Eqs. (26) and (42), we get

$$\frac{C_{D\infty}(Re^*_\infty)}{C_D(Re^*)} \equiv \left(\frac{\langle v_r\rangle}{v_{r\infty}}\right)^2 \frac{\Delta\rho g_z + M_{F\infty}}{\Delta\rho g_z(1-\langle\alpha_g\rangle) + M_F}, \quad (43)$$

where the Reynolds numbers are defined as

$$Re^*_\infty = \frac{2r_b\rho_f v_{r\infty}}{\mu_f} \quad \text{and} \quad Re^* = \frac{2\langle r_b\rangle\rho_f\langle v_r\rangle}{\mu_m}. \quad (44)$$

Now let us assume that in the Newton regime a complete similarity exists between $C_{D\infty}$ based on Re^*_∞ and C_D based on Re^* so that C_D has exactly the same functional form in terms of Re^* as $C_{D\infty}$ in terms of Re^*_∞ [4]. We also assume that $C_{D\infty}/C_D$ can be predicted by the same expression as the local constitutive relation, provided the local values of flow parameters are replaced by area-averaged values [4]. Then, we obtain

$$\langle\langle V_{gj}\rangle\rangle = (1-\langle\alpha_g\rangle)\langle v_r\rangle = v_{r\infty}(1-\langle\alpha_g\rangle)^{3/2} f(\langle\alpha_g\rangle)\frac{18.67}{1+17.67 f(\langle\alpha_g\rangle)^{6/7}}, \quad (45)$$

where $f(\langle\alpha_g\rangle)$ is defined by

$$f(\langle\alpha_g\rangle) = \frac{\mu_f}{\mu_m}\left\{\frac{\Delta\rho g_z(1-\langle\alpha_g\rangle) + M_F}{\Delta\rho g_z + M_{F\infty}}\right\}^{1/2}. \quad (46)$$

Here, μ_m/μ_f is the ratio of mixture viscosity to fluid viscosity. For $\mu_g \ll \mu_f$ the viscosity ratio is approximated by [4]

$$\frac{\mu_m}{\mu_f} = (1-\langle\alpha_g\rangle)^{-1}. \quad (47)$$

The distorted-bubbly-flow regime is characterized by the distortion of the bubble shapes and irregular motions. In this regime, the terminal velocity may be independent of bubble size [4]. From this it can be seen that the drag coefficient, $C_{D\infty}$, may not depend on the viscosity, but should be proportional to the radius of the bubble. Physically, this indicates that the drag force is governed by the distortion and swerving motion of the bubble, and the change of the bubble shape is toward an increase in the effective cross-section. Therefore, $C_{D\infty}$ should be scaled by the mean radius of the bubble rather than the Reynolds number [4]. Then,

$$C_{D\infty} = \frac{4}{3}r_b\sqrt{\frac{\Delta\rho g_z + M_{F\infty}}{\sigma}}, \quad (48)$$

where σ is the surface tension. From Eqs. (26) and (48), we get

$$v_{r\infty} = \sqrt{2}\left\{\frac{(\Delta\rho g_z + M_{F\infty})\sigma}{\rho_f^2}\right\}^{1/4}. \quad (49)$$

In considering the drag coefficient for a multi-bubble system with the same radius, we must take into account the restrictions imposed by the existence of other bubbles on the flow field [4]. Because of the random characteristics of the turbulent eddies and bubble oscillations, a bubble sees the increased drag due to other bubbles in essentially the same way as in Newton's regime for a solid-particle system where $C_{D\infty}$ is constant under a turbulent flow condition.

Hence, we postulate that, regardless of the differences in $C_{D\infty}$ in these regimes, the effect of increased drag can be predicted by the same expression [4]. Under this assumption, Eq. (45) may also be used for the distorted-bubbly-flow regime with the appropriate $v_{r\infty}$.

$$\langle\langle V_{gj}\rangle\rangle = \sqrt{2}\left\{\frac{(\Delta\rho g_z + M_{F\infty})\sigma}{\rho_f^2}\right\}^{1/4} \times \frac{18.67(1-\langle\alpha_g\rangle)^{5/2}\left\{\frac{\Delta\rho g_z(1-\langle\alpha_g\rangle)+M_F}{\Delta\rho g_z+M_{F\infty}}\right\}^{1/2}}{1+17.67(1-\langle\alpha_g\rangle)^{6/7}\left\{\frac{\Delta\rho g_z(1-\langle\alpha_g\rangle)+M_F}{\Delta\rho g_z+M_{F\infty}}\right\}^{3/7}}. \quad (50)$$

In a churn-turbulent-flow regime, some bubbles should have reached the distortion limit corresponding to the cap-bubble transition. This limit can be given by the Weber-number criterion based on the drift velocity as

$$\frac{2\rho_f\langle V_{gj}\rangle^2\langle r_b\rangle}{\sigma} = 8. \quad (51)$$

Due to the entrainment of bubbles in a wake of other bubbles and the coalescence and disintegration caused by the turbulence, the average motion of the dispersed phase is mainly governed by those bubbles that satisfy the Weber-number criterion. Thus, the drag force for a churn-turbulent flow is given by [4]

$$F_D = -\tfrac{1}{2}C'_D\rho_f\langle V_{gj}\rangle|\langle V_{gj}\rangle|\pi\langle r_b\rangle^2 \quad \text{with } C'_D = \tfrac{8}{3}. \tag{52}$$

Therefore, in a standard form,

$$F_D = -\tfrac{1}{2}C_D\rho_f\langle v_r\rangle|\langle v_r\rangle|\pi\langle r_b\rangle^2 \quad \text{with } C_D = \tfrac{8}{3}(1-\langle\alpha_g\rangle)^2. \tag{53}$$

Hence, by balancing the drag force with the pressure force, we obtain

$$\langle\langle V_{gj}\rangle\rangle = \sqrt{2}\left\{\frac{(\Delta\rho g_z + M_{F\infty})\sigma}{\rho_f^2}\right\}^{1/4} \times \left\{\frac{\Delta\rho g_z(1-\langle\alpha_g\rangle)+M_F}{\Delta\rho g_z + M_{F\infty}}\right\}^{1/4}. \tag{54}$$

When the volume of a bubble is very large, the shape of the bubble is significantly deformed to fit the channel geometry. The diameter of the bubbles becomes approximately that of the pipe with a thin liquid film separating the bubbles from the wall. The drag force for a slug flow is given by [4]

$$F_D = -\tfrac{1}{2}C_D\rho_f\langle v_r\rangle|\langle v_r\rangle|\pi\langle r_b\rangle^2 \quad \text{with } C_D = 9.8(1-\langle\alpha_g\rangle)^3. \tag{55}$$

Hence, by balancing the drag force with the pressure force and the assumed bubble radius to be $\langle r_b\rangle \approx D/2$ [4], we obtain

$$\langle\langle V_{gj}\rangle\rangle = 0.37\left[\frac{\{\Delta\rho g(1-\langle\alpha_g\rangle)+M_F\}D}{\rho_f(1-\langle\alpha_g\rangle)}\right]^{1/2}. \tag{56}$$

Then, we summarize the obtained results as follows.

Bubbly flow:

$$\langle\langle V_{gj}\rangle\rangle = \sqrt{2}\left\{\frac{(\Delta\rho g_z + M_{F\infty})\sigma}{\rho_f^2}\right\}^{1/4} \times \frac{18.67(1-\langle\alpha_g\rangle)^{5/2}\left\{\frac{\Delta\rho g_z(1-\langle\alpha_g\rangle)+M_F}{\Delta\rho g_z+M_{F\infty}}\right\}^{1/2}}{1+17.67(1-\langle\alpha_g\rangle)^{6/7}\left\{\frac{\Delta\rho g_z(1-\langle\alpha_g\rangle)+M_F}{\Delta\rho g_z+M_{F\infty}}\right\}^{3/7}}. \tag{57}$$

Slug flow:

$$\langle\langle V_{gj}\rangle\rangle = 0.37\left[\frac{\{\Delta\rho g_z(1-\langle\alpha_g\rangle)+M_F\}D}{\rho_f(1-\langle\alpha_g\rangle)}\right]^{1/2}. \tag{58}$$

Churn flow:

$$\langle\langle V_{gj}\rangle\rangle = \sqrt{2}\left\{\frac{(\Delta\rho g_z + M_{F\infty})\sigma}{\rho_f^2}\right\}^{1/4} \times \left\{\frac{\Delta\rho g_z(1-\langle\alpha_g\rangle)+M_F}{\Delta\rho g_z + M_{F\infty}}\right\}^{1/4}. \tag{59}$$

For gravity dominant flows, the above equations are simplified to Ishii's equations [4] as follows:

Bubbly flow:

$$\langle\langle V_{gj}\rangle\rangle = \sqrt{2}\left(\frac{\Delta\rho g_z\sigma}{\rho_f^2}\right)^{1/4}(1-\langle\alpha_g\rangle)^{1.75}. \tag{60}$$

Slug flow:

$$\langle\langle V_{gj}\rangle\rangle = 0.37\left(\frac{\Delta\rho g_z D}{\rho_f}\right)^{1/2}. \tag{61}$$

Churn flow:

$$\langle\langle V_{gj}\rangle\rangle = \sqrt{2}\left(\frac{\Delta\rho g_z\sigma}{\rho_f^2}\right)^{1/4}. \tag{62}$$

3.2. Annular two-phase flow

In annular two-phase flows, the relative motions between phases are governed by the interfacial geometry, the body-force field, and the interfacial momentum transfer. The constitutive equation for the gas-drift velocity in annular two-phase flows has been developed by taking into account those macroscopic effects of the structured two-phase flows. Ishii [4] derived the averaged drift velocity as

$$\overline{V_{gj}} = \langle\langle V_{gj}\rangle\rangle + (C_0-1)\langle j\rangle = \frac{1-\langle\alpha_g\rangle}{\langle\alpha_g\rangle + \left\{\frac{1+75(1-\langle\alpha_g\rangle)}{\sqrt{\langle\alpha_g\rangle}}\frac{\rho_g}{\rho_f}\right\}^{1/2}} \times \left(\langle j\rangle + \sqrt{\frac{\Delta\rho g_z D(1-\langle\alpha_g\rangle)}{0.015\rho_g}}\right). \tag{63}$$

This expression may further be simplified for $\rho_g/\rho_f \ll 1$ as

$$\overline{V_{gj}} \approx \frac{1-\langle\alpha_g\rangle}{\langle\alpha_g\rangle + 4\sqrt{\rho_g/\rho_f}}\left(\langle j\rangle + \sqrt{\frac{\Delta\rho g_z D(1-\langle\alpha_g\rangle)}{0.015\rho_g}}\right). \tag{64}$$

4. Distribution parameter

4.1. Dispersed two-phase flow

Ishii [4] developed a simple correlation for the distribution parameter in bubbly-flow regime. Ishii first considered a fully developed bubbly flow and assumed that the distribution parameter would depend on the density ratio, ρ_g/ρ_f and on the Reynolds number, *Re* defined by $\langle j_f\rangle D/v_f$. As the density ratio approaches unity, the distribution parameter should become unity.

Based on the limit and various experimental data in fully developed flows, the distribution parameter was given approximately by

$$C_0 = C_\infty(Re) - \{C_\infty(Re) - 1\}\sqrt{\rho_g/\rho_f}, \tag{65}$$

where C_∞ is the asymptotic value of C_0. Here, the density group scales the inertia effects of each phase in a transverse void distribution. Physically, Eq. (65) models the tendency of the lighter phase to migrate into a higher-velocity region, thus resulting in a higher void concentration in the central region.

For a laminar flow, $C_{\infty,l}$ is 2 [4], but due to the large velocity gradient, C_0 is very sensitive to $\langle\alpha_g\rangle$ at low void fractions. Recently, Hibiki and Ishii [10] developed $C_{\infty,t}$ correlation in a turbulent bubbly flow as

$$C_{\infty,t} = 1.2\{1 - \exp(-22\langle D_{Sm}\rangle/D)\}, \tag{66}$$

where D_{Sm} is the bubble Sauter mean diameter, which can be predicted by the following correlation [11].

$$\widetilde{D}_{Sm} = 1.99\widetilde{Lo}^{-0.335}\widetilde{Re}^{-0.239}, \tag{67}$$

where $\widetilde{D}_{Sm} \equiv \langle D_{Sm}\rangle/Lo$, $Lo \equiv \sqrt{\sigma/(g\Delta\rho)}$, $\widetilde{Lo} \equiv Lo/D_H$ and $\widetilde{Re} \equiv (\langle\varepsilon\rangle^{1/3}Lo^{1/3})Lo)/\nu_f$. The energy dissipation rate per unit mass, ε, can be given by

$$\langle\varepsilon\rangle = g\langle j_g\rangle \exp(-0.000584Re) + \frac{\langle j\rangle}{\rho_m}\left(-\frac{dp}{dz}\right)_F \times \{1 - \exp(-0.000584Re)\}. \tag{68}$$

The pressure loss per unit length due to friction can be calculated from Lockhart-Martinelli's correlation [12]. The applicability of Eq. (66) has been confirmed for the experimental conditions such as $0.262 \leqslant \langle j_f\rangle \leqslant 5.00$ m/s, $25.4 \leqslant D \leqslant 60$ mm, and 1.40 mm $\leqslant \langle D_{Sm}\rangle$. Since Eq. (66) is rather complicated and its applicability is limited by the validated experimental range, $C_{\infty,t} = 1.2$ proposed by Ishii [4] or $C_{\infty,t} = 1.05$ based on available distribution parameters determined by local flow measurements [10] may still be utilized by accepting a certain prediction error for simplicity.

Taking account of the flow transition from a laminar flow to a turbulent flow, C_∞ in bubbly-flow regime may be approximated by

$$C_\infty = C_{\infty,l}\exp(cRe) + C_{\infty,t}\{1 - \exp(cRe)\}, \tag{69}$$

The coefficient, c, may roughly be estimated to be -0.000584 by the condition of $\exp(cRe) = 0.5$ at $Re = 1189$. Thus,

$$C_\infty = 2.0\exp(-0.000584Re) + 1.2\{1 - \exp(-22\langle D_{Sm}\rangle/D)\} \times \{1 - \exp(-0.000584Re)\}. \tag{70}$$

Experimental data suggest that C_∞ in slug, and churn flows may be approximated to be 1.2 [4]. Then, we obtain the following results.

Bubbly flow:

$$C_0 = 2.0\exp(-0.000584Re) + 1.2\{1 - \exp(-22\langle D_{Sm}\rangle/D)\} \times \{1 - \exp(-0.000584Re)\} - [2.0\exp(-0.000584Re) + 1.2\{1 - \exp(-22\langle D_{Sm}\rangle/D)\} \times \{1 - \exp(-0.000584Re)\} - 1]\sqrt{\frac{\rho_g}{\rho_f}}. \tag{71}$$

Slug flow:

$$C_0 = 1.2 - 0.2\sqrt{\rho_g/\rho_f}. \tag{72}$$

Churn flow:

$$C_0 = 1.2 - 0.2\sqrt{\rho_g/\rho_f}. \tag{73}$$

The validity of the above equations has been confirmed in the previous studies [4,10].

4.2. Annular two-phase flow

In separated flows, local relative velocity between two phases can not be defined. If small liquid droplets are entrained in the gas core or small gas bubbles are entrained in the liquid film, local relative velocity may be approximated to be zero, resulting in $\langle\langle V_{gj}\rangle\rangle \approx 0$. Thus, we have

$$C_0 \approx \frac{1 - \langle\alpha_g\rangle}{\langle\alpha_g\rangle + \left\{\frac{1+75(1-\langle\alpha_g\rangle)}{\sqrt{\langle\alpha_g\rangle}}\frac{\rho_g}{\rho_f}\right\}^{1/2}}\left(1 + \frac{\sqrt{\frac{\Delta\rho\, g_z D(1-\langle\alpha_g\rangle)}{0.015\rho_g}}}{\langle j\rangle}\right) + 1. \tag{74}$$

This expression may further be simplified for $\rho_g/\rho_f \ll 1$ as

$$C_0 \approx \frac{1 - \langle\alpha_g\rangle}{\langle\alpha_g\rangle + 4\sqrt{\rho_g/\rho_f}}\left(1 + \frac{\sqrt{\frac{\Delta\rho\, g_z D(1-\langle\alpha_g\rangle)}{0.015\rho_g}}}{\langle j\rangle}\right) + 1. \tag{75}$$

The validity of the above equation has been confirmed in the previous study [4].

5. Results and discussions

5.1. Example computation of newly developed one-dimensional drift velocity

In this section, an example computation of the newly developed constitutive equations for one-dimensional drift velocity will be performed for dispersed two-phase flows. The figure at the upper left of Fig. 1 shows an example computation of the newly developed constitutive equations for one-dimensional drift velocity in the $\langle j_f\rangle$ vs. $\langle\langle V_{gj}\rangle\rangle$ plane. The computational conditions are

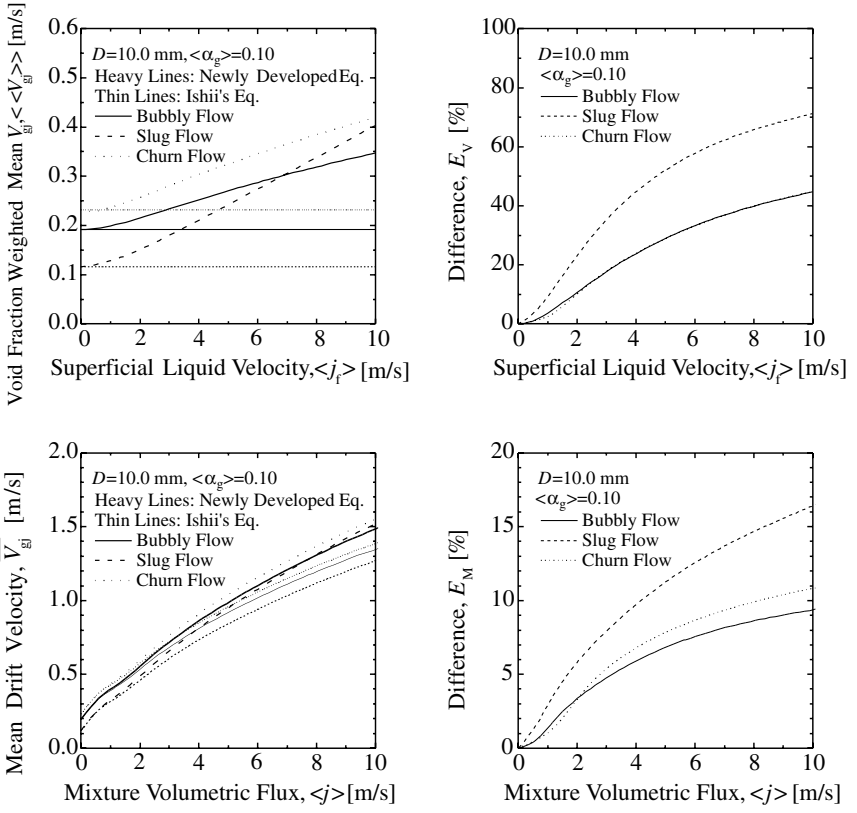

Fig. 1. Example computation of newly developed constitutive equations for drift velocity.

$D = 10.0$ mm and $\langle \alpha_g \rangle = 0.10$. The value of $D = 10.0$ mm is about the hydraulic equivalent diameter of the flow channel in 17×17 bundle PWR fuel assembly or 9×9 bundle BWR fuel assembly. Heavy solid, broken and dotted lines indicate the void-fraction-weighted mean drift velocity calculated from the newly developed equations for bubbly, slug, and churn flows, respectively. On the other hand, thin solid, broken and dotted lines indicate the void-fraction-weighted mean drift velocity calculated from Ishii's equations [4] for bubbly, slug, and churn flows, respectively. The values of $\langle\langle V_{gj} \rangle\rangle$ calculated by Ishii's equations are independent of the superficial liquid velocity, whereas the values calculated by the newly developed equations are increased by the superficial liquid velocity due to the increased frictional pressure gradient. The figure at the upper right of Fig. 1 shows the difference between $\langle\langle V_{gj} \rangle\rangle$ calculated by the newly developed equations and Ishii's equations for the example computation shown in the figure at the upper left. The difference between $\langle\langle V_{gj} \rangle\rangle$ calculated by the newly developed equations and Ishii's equations is defined by

$$E_V\ [\%] = \frac{|\langle\langle V_{gj} \rangle\rangle - \langle\langle V_{gj} \rangle\rangle_{\text{Ishii}}|}{\langle\langle V_{gj} \rangle\rangle} \times 100, \tag{76}$$

where the subscript of Ishii means the value calculated by Ishii's equation for respective flow regime. In bubbly-flow and churn-flow regimes, the difference between $\langle\langle V_{gj} \rangle\rangle$ calculated by the newly developed equations and Ishii's equations for $\langle j_f \rangle \leqslant 2.0$ m/s and $\langle j_f \rangle \leqslant 3.3$ m/s are estimated to be within $\pm 10\%$ and $\pm 20\%$, respectively. In slug-flow regime, the difference between $\langle\langle V_{gj} \rangle\rangle$ calculated by the newly developed equations and Ishii's equations for $\langle j_f \rangle \leqslant 1.0$ m/s and $\langle j_f \rangle \leqslant 1.7$ m/s are estimated to be within $\pm 10\%$ and $\pm 20\%$, respectively. Thus, for relatively low liquid velocity, the difference between $\langle\langle V_{gj} \rangle\rangle$ calculated by the newly developed equations and Ishii's equations is insignificant. In such flow conditions, Ishii's equations, which is the approximate form of the newly developed equations, give fairly good estimations of $\langle\langle V_{gj} \rangle\rangle$ as already proved experimentally [4,10].

The figure at the lower left of Fig. 1 shows an example computation of the newly developed constitutive equations for one-dimensional drift velocity in the $\langle j_f \rangle$ vs. $\overline{V_{gj}}$ plane. Heavy solid, broken and dotted lines indicate the mean drift velocity calculated by Eq. (9) with the newly developed equations for bubbly, slug, and churn flows, respectively. On the other hand, thin solid, broken and dotted lines indicate the mean drift velocity calculated by Eq. (9) with Ishii's equations [4] for

bubbly, slug, and churn flows, respectively. In this example computation, Eq. (71) is expansively used for the estimation of the distribution parameter for bubbly-flow regime. As can be seen from Eq. (71), the distribution parameter is dependent on the superficial liquid velocity. For example, as the superficial liquid velocity increases from 0.50 to 10 m/s keeping the void fraction at 0.10, the value of the distribution parameter for bubbly-flow regime estimated by Eq. (71) decreases from 1.24 to 1.11. This tendency agrees with the experimental observation such that the void fraction distribution becomes flatter for higher liquid velocity [13]. Eqs. (72) and (73) are used for the estimations of the distribution parameters for slug-flow and churn-flow regimes, respectively. Since the values of the distribution parameter for all flow regimes tested in this calculation are larger than unity, the values of $\overline{V_{gj}}$ are increased by increasing the mixture volumetric flux (see Eq. (9)). The figure at the lower right of Fig. 1 shows the difference between $\overline{V_{gj}}$ calculated by the newly developed equations and Ishii's equations for the example computation shown in the figure at the lower left. The difference between $\overline{V_{gj}}$ calculated by the newly developed equations and Ishii's equations is defined by

$$E_{\mathrm{M}}\ [\%] = \frac{|\overline{V_{gj}} - \overline{V_{gj\mathrm{Ishii}}}|}{\overline{V_{gj}}} \times 100. \tag{77}$$

In bubbly-flow and churn-flow regimes, the difference between $\overline{V_{gj}}$ calculated by the newly developed equations and Ishii's equations is about ±10% even for high mixture volumetric flux such as $\langle j\rangle = 10$ m/s. In slug-flow regime, the difference between $\overline{V_{gj}}$ calculated by the newly developed equations and Ishii's equations is lower than ±10% for $\langle j\rangle \leqslant 4.18$ m/s. Since the term of $(C_0 - 1)\langle j\rangle$ for slug-flow and churn-flow regimes is dominant in determining $\overline{V_{gj}}$ for high mixture volumetric flux, the prediction error in $\langle\langle V_{gj}\rangle\rangle$ may not affect the prediction error in $\overline{V_{gj}}$ significantly. As a consequence, for slug-flow and churn-flow regimes Ishii's equations, which is the approximate form of the newly developed equations, give fairly good estimations of $\overline{V_{gj}}$ even for relatively high mixture volumetric flux. However, in bubbly-flow regime, the distribution parameter can be unity or negative. Thus, since the term of $(C_0 - 1)\langle j\rangle$ for bubbly-flow regime can be comparable to $\langle\langle V_{gj}\rangle\rangle$ even for high mixture volumetric flux, the prediction error in $\overline{V_{gj}}$ may reach the prediction error in $\langle\langle V_{gj}\rangle\rangle$, see figure at the upper right of Fig. 1.

5.2. Verification of newly developed constitutive equations for drift velocity

An accurate measurement of the relative velocity between phases in various flow regimes is indispensable to evaluate the newly developed constitutive equations for drift velocity experimentally. However, no data bases on the relative velocity except bubbly-flow regime are available due to the difficulty of the accurate measurement. The contribution of the drift velocity to the gas velocity or the contribution of $\langle\langle V_{gj}\rangle\rangle$ to $\overline{V_{gj}}$ would be rather small for flow regimes such as slug, churn, and annular flow regimes, whereas it would be significant for bubbly-flow regime. Thus, it is important to evaluate the newly developed constitutive equations for drift velocity, particularly, in bubbly-flow regime with drift velocities determined from measured local flow parameters. Although several data bases in bubbly-flow regime are available for relatively low superficial liquid velocity such as $\langle j_{\mathrm{f}}\rangle \leqslant 1.4$ m/s [10], only two data bases in bubbly-flow regime [13,14] are available for relatively high liquid velocity such as $\langle j_{\mathrm{f}}\rangle \geqslant 2.0$ m/s where the difference between the drift velocities calculated by the newly developed equations and Ishii's equations will be marked.

These two data bases were obtained by the present authors at the Thermal-hydraulics and Reactor Safety Laboratory in Purdue University [13,14]. The present authors measured local flow parameters of adiabatic air-water bubbly flows in vertical pipes with inner diameters of 25.4 and 50.8 mm. Local measurements of void fraction and gas velocity were performed by using the double sensor probe method. On the other hand, local measurement of liquid velocity was conducted by using hotfilm anemometry. Data was taken at three different axial locations as well as fifteen radial positions. For $D = 25.4$ mm, a total of 75 ($=25\times3$) data sets were acquired consisting of 25 flow conditions and 3 axial locations ($z/D = 12.0$, 65.0, and 125) [14], and for $D = 50.8$ mm, a total of 54 ($=18\times3$) data sets were acquired consisting of 18 flow conditions and 3 axial locations ($z/D = 6.00$, 30.3, and 53.5) [13]. Thus, data sets in developing and fully-developed flows are available. The detailed discussions of local flow parameters are found in our previous papers [13,14].

Figs. 2 and 3 show the comparisons of drift velocities predicted for bubbly and slug flows with the drift velocities determined by Eq. (10) from local parameters of fully-developed flows measured at $z/D = 125$ in the 25.4-mm diameter pipe and at $z/D = 53.5$ in the 50.8-mm diameter pipe, respectively. In these figures, the solid and broken lines indicate the drift velocities calculated by the newly developed equations and Ishii's equations, respectively. Unfortunately, the scatter of data points appears to be rather large for relatively high liquid velocity where the difference between the drift velocities calculated by the newly developed equations and Ishii's equations will be marked. As can be seen from Eqs. (8) and (10), the uncertainty of the void-fraction-weighted mean drift velocity estimated from the measurement would mainly be attributed to the measurement error of the relative velocity between phases, which can be calculated by subtracting the liquid velocity from the gas velocity. When the measurement errors for gas and liq-

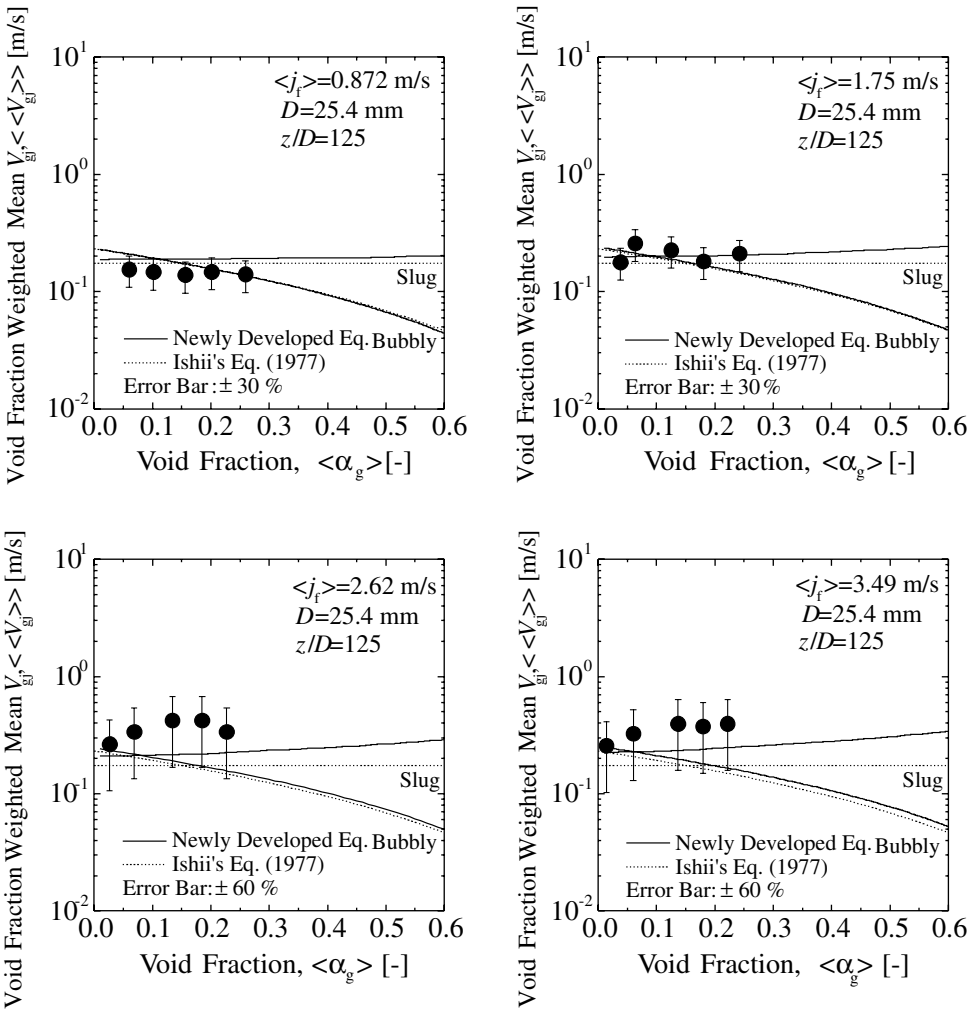

Fig. 2. Comparison of newly developed constitutive equations for drift velocity with experimental drift velocities obtained in fully-developed bubbly flows in a 25.4-mm diameter pipe [14].

uid velocities are ±10%, the uncertainty in the void-fraction-weighted mean drift velocity can roughly be estimated to be ±40%, ±80%, and ±400% for the gas velocities of 0.5, 1, and 5 m/s, respectively, from the error propagation. Here, the void-fraction-weighted mean drift velocity is assumed to be 0.25 m/s in the error estimation by conservative estimate. Thus, it would be very difficult to make a quantitative discussion based on the data for $\langle j_f \rangle \geqslant 1.0$ m/s due to considerably large error. As an indication of the measurement error, the error bars for ±30% for relatively low velocity such as $\langle j_f \rangle < 2.0$ m/s and for ±60% for relatively high velocity such as $\langle j_f \rangle \geqslant 2.0$ m/s are shown in the figures.

As can be seen from Figs. 2 and 3, the measured void-fraction-weighted mean drift velocities for relatively low liquid velocities such as $\langle j_f \rangle < 2.0$ m/s appear to decrease with the increase in the void fraction. As expected from the example computation discussed in the previous section, the differences between the drift velocities in bubbly-flow regime calculated by the newly developed equation and Ishii's equation are rather small, and both equations can represent the dependence of the drift velocity on the void fraction marvelously. For higher liquid velocities such as $\langle j_f \rangle \geqslant 2.0$ m/s and $\langle \alpha_g \rangle \geqslant 0.15$, the measured void-fraction-weighted mean drift velocities come to agree with the calculated drift velocities in slug-flow regime rather than the calculated drift velocities in bubbly-flow regime. This may be attributed to the flow regime transition from bubbly flow to slug flow. It was observed experimentally that the formation of cap bubbles was initiated at $\langle \alpha_g \rangle = 0.15$ for relatively high liquid velocity due to strong bubble-bubble interaction [13,14]. Although the measurement errors in the drift velocity are considerable for relatively high liquid velocity, the newly

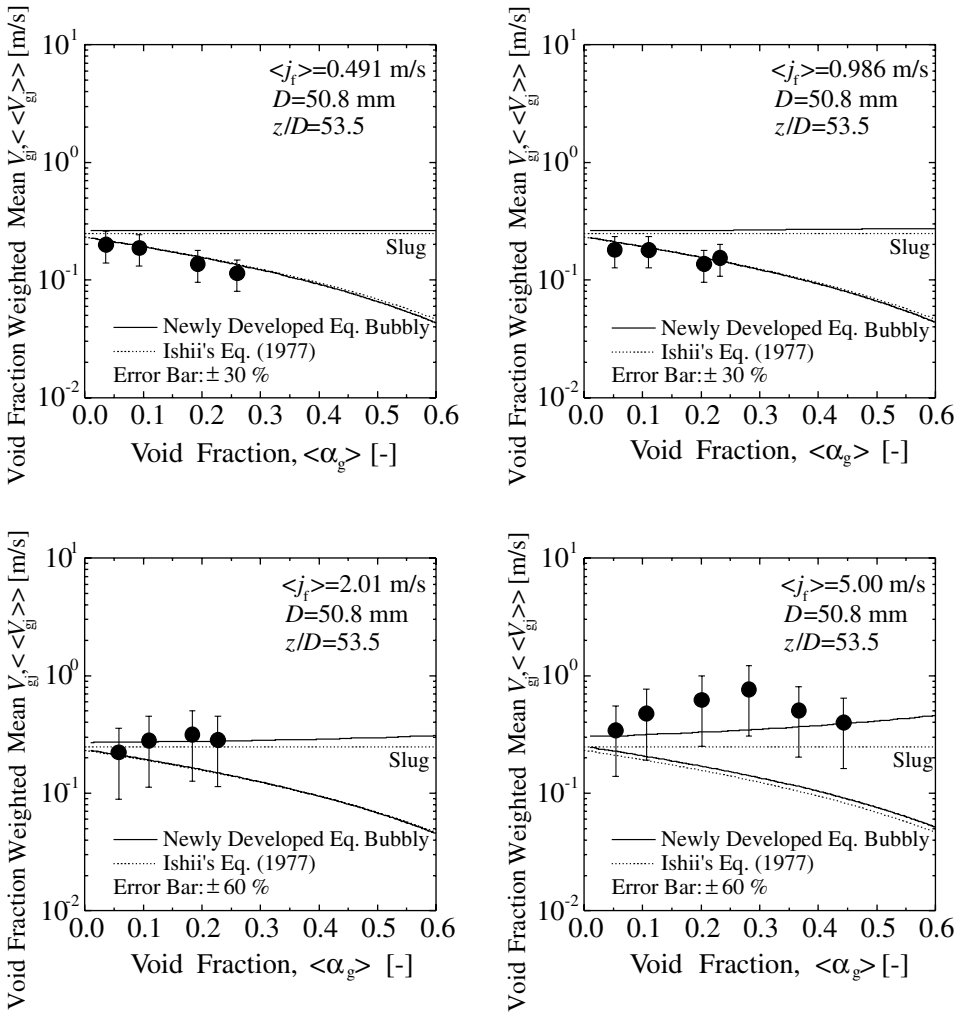

Fig. 3. Comparison of newly developed constitutive equations for drift velocity with experimental drift velocities obtained in fully-developed bubbly flows in a 50.8-mm diameter pipe [13].

developed equation for slug-flow regime seems to give predictions for the measured drift velocities better than the approximated form of the newly developed equation, namely Ishii's equation.

Fig. 4 shows the example comparisons of drift velocities predicted for bubbly and slug flows with the drift velocities determined by Eq. (10) from local parameters of developing flows measured at $z/D = 6.00$ in a 50.8-mm diameter pipe. In the figure, the solid and broken lines indicate the drift velocities calculated by the newly developed equations and Ishii's equations, respectively. As an indication of the measurement error, the error bars for ±30% for relatively low liquid velocity such as $\langle j_f \rangle < 2.0$ m/s and for ±60% for relatively high liquid velocity such as $\langle j_f \rangle \geqslant 2.0$ m/s are shown in the figure. Similarly to the fully-developed flows, the differences between the drift velocities in bubbly-flow regime calculated by the newly developed equation and Ishii's equation are rather small for relatively low liquid velocities such as $\langle j_f \rangle < 2.0$ m/s, and both equations can represent the dependence of the drift velocity on the void fraction marvelously. For higher liquid velocities such as $\langle j_f \rangle \geqslant 2.0$ m/s and $\langle \alpha_g \rangle \geqslant 0.15$, the measured void-fraction-weighted mean drift velocities come to agree with the calculated drift velocities in slug-flow regime rather than the calculated drift velocities in bubbly-flow regime. Although the measurement errors in the drift-velocity are considerable for relatively high liquid velocity, the newly developed equation for slug-flow regime seems to give predictions for the measured drift velocities better than the approximated form of the newly developed equation, namely Ishii's equation. Thus, it may be concluded that the newly developed equations can be applicable even to a developing flow.

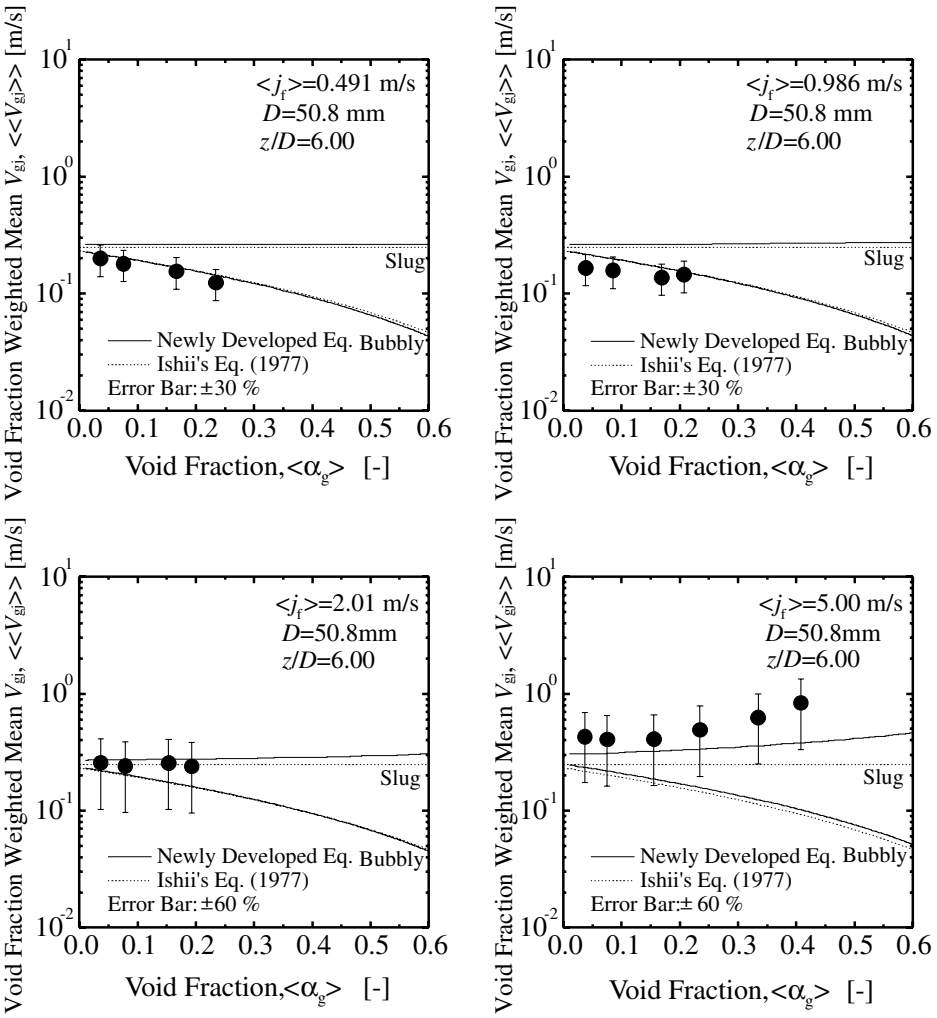

Fig. 4. Comparison of newly developed constitutive equations for drift velocity with experimental drift velocities obtained in developing bubbly flows in a 50.8-mm diameter pipe [13].

The effect of the wall friction on the drift velocity would be significant for some extreme flow conditions such as very high liquid flow and microgravity conditions. Thus, the precise formulation of the drift velocity presented in this study will be important for such extreme flow conditions. In order to reevaluate the newly developed constitutive equations for drift velocity, extensive experimental works to obtain accurate data bases for such extreme flow conditions should be addressed in the future study.

6. Conclusions

In view of the practical importance of the drift-flux model for two-phase flow analysis in general and in the analysis of nuclear-reactor transients and accidents in particular, the distribution parameter and the drift velocity have been studied for various flow regimes. The obtained results are as follows:

(1) The constitutive equations that specify the distribution parameter in various flow regimes have been discussed briefly.
(2) The constitutive equations that specify the relative motion between phases in various flow regimes have been derived by taking into account the effect of the wall friction on the relative velocity between phases.
(3) The example computation of the newly developed constitutive equations for drift velocity has been performed, and the newly developed equations have been compared with the approximated form of the newly developed equations, namely Ishii's equations.

(4) A comparison of the newly developed constitutive equations for drift velocity with fully-developed bubbly-flow data shows a satisfactory agreement. It has also been confirmed experimentally that the newly developed equations can be applicable to developing bubbly flows.
(5) For relatively low liquid velocity conditions, the difference between the drift velocity calculated by the newly developed equations and Ishii's equation is insignificant, whereas the difference comes to be significant for relatively high liquid velocity conditions. The example computation for $D = 10.0$ mm and $\langle \alpha_g \rangle = 0.10$ indicates that the difference reaches to 70% at $\langle j_f \rangle = 10$ m/s.

Acknowledgements

The authors wish to thank Prof. J.Y. Lee (Handong Global University, South Korea) for his fruitful discussion. Part of this work was supported by the Grant-in-Aid for Scientific Research from the Ministry of Education, Science, Sport and Culture (no.: 14580542).

References

[1] J.M. Delhaye, Equations fondamentales des écoulements diphasiques, Part 1 and 2, CEA-R-3429, France, 1968.
[2] M. Ishii, Thermo-fluid Dynamic Theory of Two-phase Flow, Eyrolles, Paris, 1975.
[3] N. Zuber, J.A. Findlay, Average volumetric concentration in two-phase flow systems, J. Heat Transfer 87 (1965) 453–468.
[4] M. Ishii, One-dimensional drift-flux model and constitutive equations for relative motion between phases in various two-phase flow regimes, ANL-77-47, USA, 1977.
[5] M. Ishii, Thermally-induced flow instabilities in two-phase mixtures in thermal equilibrium, Ph.D. Thesis, Georgia Institute of Technology, GA, USA, 1971.
[6] A. Tomiyama, I. Kataoka, I. Zun, T. Sakaguchi, Drag coefficients of single bubble under normal and micro gravity conditions, JSME Int. J. Ser. B 41 (1998) 472–479.
[7] R. Clift, J.R. Grace, M.E. Weber, Bubbles, Drops, and Particles, Academic Press, New York, USA, 1978.
[8] M. Ishii, K. Mishima, Two-fluid model and hydrodynamic constitutive relations, Nucl. Eng. Des. 82 (1984) 107–126.
[9] A. Serizawa, I. Kataoka, I. Michiyoshi, Turbulence structure of air–water bubbly flow—II. Local properties, Int. J. Multiphase Flow 2 (1975) 235–246.
[10] T. Hibiki, M. Ishii, Distribution parameter and drift velocity of drift-flux model in bubbly flow, Int. J. Heat Mass Transfer 45 (2002) 707–721.
[11] T. Hibiki, M. Ishii, Interfacial area concentration of bubbly flow systems, Chem. Eng. Sci. 57 (2002) 3967–3977.
[12] R.W. Lockhart, R.C. Martinelli, Proposed correlation of data for isothermal two-phase, two-component flow in pipes, Chem. Eng. Prog. 5 (1949) 39–48.
[13] T. Hibiki, M. Ishii, Z. Xiao, Axial interfacial area transport of vertical bubbly flows, Int. J. Heat Mass Transfer 44 (2001) 1869–1888.
[14] T. Hibiki, M. Ishii, Experimental study on interfacial area transport in bubbly two-phase flows, Int. J. Heat Mass Transfer 42 (1999) 3019–3035.